nature materials

ARTICLES

PUBLISHED ONLINE: 10 NOVEMBER 2014 | DOI: 10.1038/NMAT4138

Orbital-driven nematicity in FeSe

S-H. Baek[1]*, D. V. Efremov[1], J. M. Ok[2], J. S. Kim[2], Jeroen van den Brink[1,3] and B. Büchner[1,3]

A fundamental and unconventional characteristic of superconductivity in iron-based materials is that it occurs in the vicinity of two other instabilities. In addition to a tendency towards magnetic order, these Fe-based systems have a propensity for nematic ordering: a lowering of the rotational symmetry while time-reversal invariance is preserved. Setting the stage for superconductivity, it is heavily debated whether the nematic symmetry breaking is driven by lattice, orbital or spin degrees of freedom. Here, we report a very clear splitting of NMR resonance lines in FeSe at $T_{nem} = 91$ K, far above the superconducting T_c of 9.3 K. The splitting occurs for magnetic fields perpendicular to the Fe planes and has the temperature dependence of a Landau-type order parameter. Spin–lattice relaxation rates are not affected at T_{nem}, which unequivocally establishes orbital degrees of freedom as driving the nematic order. We demonstrate that superconductivity competes with the emerging nematicity.

Even if the existence of nematic order in the different classes of iron-based superconductors is by now a well-established experimental fact, its origin remains controversial[1–7]. It is related either to a lattice instability that causes a regular structural phase transition, to the formation of time-reversal-invariant magnetic order, for instance an Ising spin-nematic[8–10] state, or to the ordering of orbital degrees of freedom[11–15]. As the nematic instability is a characteristic feature of the normal state from which at lower temperatures the superconductivity emerges, the different possible microscopic origins of nematicity are directly linked to the properties of the superconducting state[16,17]. From a symmetry point of view it is clear that when one of these three orderings (lattice/spin/orbital) develops, it must affect the other two—the crucial challenge thus lies in establishing which ordering is primary, and to determine to which extent this primary order affects the two other degrees of freedom. It has been established that the lattice distortion, which at T_{nem} reduces the crystallographic symmetry from tetragonal to orthorhombic, is an unlikely primary order parameter, not only because the distortion is weak, but also because measurements of the resistance anisotropy have shown that the structural distortion is a conjugate field to a primary order parameter, therefore not the order parameter itself[2]. This basically restricts the driving force for the nematicity to be of electronic origin: either due the electron's spin or its orbital degree of freedom.

FeSe is an attractive iron-based superconductor to study this issue, as it is a binary system with a rather simple structure (see Fig. 1), while sharing many common features with other Fe-based superconductors[18]. Our bulk FeSe single crystals undergo a clear tetragonal to orthorhombic transition at $T_{nem} = 91$ K and at $T_c = 9.3$ K superconductivity sets in, which is consistent with previous reports[5]. In single-layer FeSe films a much higher T_c has been reported, 65 K (refs 19–23) and above[24], which is even higher than in any other iron-based superconductor. The high quality of our FeSe single crystals is confirmed by their very sharp superconducting transition and large residual resistivity ratio (see Supplementary Methods).

To establish whether spins or orbitals are responsible for its nematic instability we have measured ^{77}Se NMR spectra as a function of temperature. The Se atoms in FeSe sit centrally above and below the Fe_4 plaquettes that form an almost square lattice (see Fig. 1b). For the NMR measurements we used an external field $H = 9$ T applied in a direction either parallel or perpendicular to the crystallographic c axis, which is normal to the Fe planes (Fig. 1a). In the high-temperature tetragonal phase the spectra are extremely narrow with the full-width at half-maximum of $\sim$1 kHz for $H \parallel a$ and $\sim$1.5 kHz for $H \parallel c$, which is characteristic of a highly homogeneous sample (see Fig. 2). Below T_{nem} we observe that the ^{77}Se line splits into two lines with equal spectral weight for in-plane fields, $H \parallel a$. Note that in the orthorhombic phase our crystal is fully twinned. The notation $H \parallel a$ thus means that actually one type of domain in the crystal experiences a magnetic field $H \parallel a$ and the other type of domain has $H \parallel b$. These two domains occur with equal probability. We shall refer to the split lines as l_1 and l_2 with frequency ν_1 and ν_2, respectively ($\nu_1 < \nu_2$). In contrast, the ^{77}Se spectrum for $H \parallel c$ consists of a single line l_3 at frequency ν_3 that does not split and remains narrow down to low temperatures. From this, one can already conclude that the l_1–l_2 line splitting must be the consequence of an in-plane symmetry change.

We note that the ^{77}Se nuclear spin is 1/2 so that the observed splitting cannot be due to a quadrupolar-type coupling to local lattice distortions. This is in contrast to LaFeAsO, in which the quadrupolar splitting of the ^{75}As line in twinned single crystals for $H \perp c$ reflects the presence of orthorhombic domains[7]. On two further grounds it can be excluded that the orthorhombic lattice distortion causes the l_1–l_2 splitting. First, the splitting changes significantly when FeSe enters the superconducting state (see Fig. 3b), where the lattice structure does not change notably[25]. That the splitting is of electronic origin is attested also by a more detailed consideration of the temperature dependence of the resonance frequency ν_i ($i = 1 \ldots 3$) for each of the three NMR lines. The T dependence is shown in Fig. 2 in terms of the Knight shift $\mathcal{K}_i = (\nu_i - \nu_0)/\nu_0$ of ν_i away from an isolated nucleus ($\nu_0 = \gamma_n H$ with the nuclear gyromagnetic ratio γ_n). In a paramagnetic state $\mathcal{K} = A_{hf}\chi_{spin} + \mathcal{K}_{chem}$ so that $\mathcal{K}$ is directly related to the local spin susceptibility χ_{spin}. Here A_{hf} is the hyperfine coupling constant and $\mathcal{K}_{chem}$ is the temperature-independent chemical shift. It is clear that the splitting between l_3 and the degenerate l_1, l_2 pair in the tetragonal structure (that is, for $T > T_{nem}$) is caused by the in-plane ($\|a$)–out-of-plane ($\|c$) anisotropy of the hyperfine

[1]IFW Dresden, Helmholtzstr. 20, 01069 Dresden, Germany, [2]Department of Physics, Pohang University of Science and Technology, Pohang 790-784, Korea, [3]Department of Physics, Technische Universität Dresden, 01062 Dresden, Germany. *e-mail: sbaek.fu@gmail.com

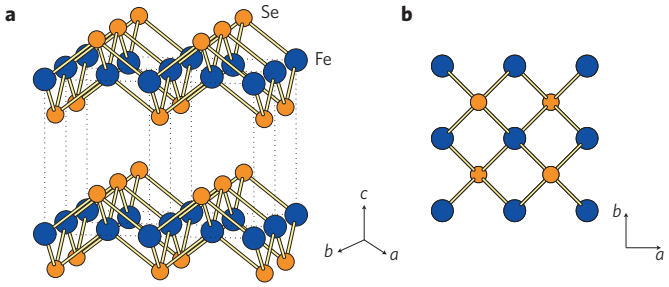

Figure 1 | Schematic crystallographic structure of FeSe. a,**b**, Fe–Se layers stacked along the *c* direction (**a**) and the in-plane Fe atoms forming an almost square lattice with Se atoms centred alternatively above and below Fe_4 plaquettes (**b**).

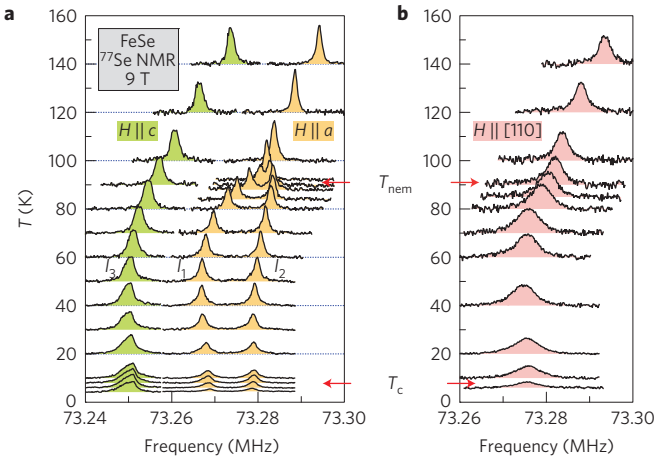

Figure 2 | ^{77}Se NMR spectra for the FeSe single crystal. a, Measured at a field of 9 T applied parallel to either the crystallographic *a* axis or *c* axis, as a function of temperature. The ^{77}Se line splits into two lines (l_1 and l_2) at $T_{nem} = 91$ K for $H \| a$, whereas the line l_3 for $H \| c$ remains narrow at all temperatures. To avoid an overlap, the spectra for $H \| c$ are offset by −10 kHz. **b**, For an in-plane magnetic field where $H \| [110]$. The absence of the line splitting for this field orientation is direct proof for a breaking of the local four-fold rotational symmetry. The broadening of the line is attributed to the strain induced by glueing this crystal inside the NMR coil.

coupling and the spin susceptibility. This anisotropy is caused by the crystallographic structure being very different in the directions $\|a$ and $\|c$, owing to the manifestly layered lattice structure of FeSe. From the data in Fig. 3a it is clear that the l_3–$l_{1,2}$ splitting $\nu_3 - \nu_{1,2}$ above T_{nem} is similar in size to the l_2–l_1 splitting $\Delta\nu = \nu_2 - \nu_1$ in the low-temperature orthorhombic state. It is evident that such a very large splitting $\Delta\nu$ cannot be caused by the small lattice displacements in the orthorhombic state, involving atoms that move distances less than 0.5% of the lattice constant[5,25]. This is exemplified by the average $\mathcal{K}^{av}_{\|a} = (\mathcal{K}_1 + \mathcal{K}_2)/2$ of the two $H \| a$ and $H \| b$ lines (for the two different orthorhombic domains) having the same temperature dependence as $\mathcal{K}_{\|c} = \mathcal{K}_3$ in the entire temperature range. This is very different from the behaviour of the Knight shift splitting $\Delta\mathcal{K}_{\|a} = (\mathcal{K}_2 - \mathcal{K}_1)/2 \propto \Delta\nu$ between l_2 and l_1 below T_{nem}. From the temperature dependence of $\Delta\mathcal{K}_{\|a}$ (shown in Fig. 3b), one sees that it exhibits the typical $\sqrt{T_{nem} - T}$ behaviour of a Landau-type order parameter close to a second-order phase transition.

Having established an order parameter type of behaviour of splitting $\Delta\nu$ and having excluded it is of lattice origin, we consider next the possibility that spin degrees of freedom cause the observed in-plane anisotropy of the Knight shift in the orthorhombic state. We have therefore measured the spin–lattice relaxation rate T_1^{-1} as a function of temperature (see Fig. 3). The quantity $(T_1T)^{-1}$ is proportional to the $\mathbf{q}$-sum of the imaginary part of the dynamical susceptibility, that is, $(T_1T)^{-1} \propto \sum_{\mathbf{q}} A^2_{hf}(\mathbf{q})\chi''(\mathbf{q},\omega)/\omega$, thereby probing antiferromagnetic (AFM) spin fluctuations. We observe that when crossing the nematic phase transition, $(T_1T)^{-1}$ barely changes, indicating that AFM fluctuations are not enhanced around T_{nem} and the system is evidently very far away from any magnetic instability. Only when further lowering the temperature we observe that $(T_1T)^{-1}$ gradually increases and that at T_c, when superconductivity sets in, the AFM fluctuations are significantly enhanced. This observation is in agreement with previous $(T_1T)^{-1}$ measurements on FeSe powders[26] and evidences that spin fluctuations are not driving the nematic transition. Moreover, the extremely narrow ^{77}Se NMR lines being well preserved down to 4.2 K indicates the complete absence of static magnetism[27].

The remaining degree of freedom that can drive the nematic ordering is the orbital one, in particular in the form of ferro-orbital order (FOO). It is clear that such an orbital ordering breaks the in-plane local symmetry at the Se sites (see Fig. 4), and generates two non-equivalent directions $\perp c$: the *a* and *b* direction. We first consider FOO from a theoretical point of view, defining the FOO order parameter as $\psi = (n_x - n_y)/(n_x + n_y)$, where $n_{x,y}$ corresponds to the occupation of $x = d_{xz}$ and $y = d_{yz}$ orbitals indicated in Fig. 4 (z corresponds to the crystallographic *c* axis). Given the symmetries of the system, the free energy in the vicinity of the orbital ordering transition in the presence of a magnetic field $\mathbf{H}$ can be expanded as:

$$F = \frac{a}{2}\psi^2 + \frac{b}{4}\psi^4 + \frac{1}{2\chi_\perp}M^2 - \gamma\psi(M_x^2 - M_y^2) + \frac{g}{2}M_z^2 + \mathbf{MH} \quad (1)$$

where $\mathbf{M}$ is the magnetic moment. An important quantity is γ, the coupling between the orbital order parameter and magnetization. For localized 3*d* states it is perturbatively related to the strength of spin–orbit interaction λ and energy difference Δ_d between the x and y, z states as $\gamma \propto \lambda^2/\Delta_d$. From equation (1) one obtains susceptibilities of the form $\chi_{xx,yy} = \chi_\perp/(1 \pm \gamma\psi\chi_\perp) \approx \chi_\perp(1 \mp \gamma\psi\chi_\perp)$ and $\chi_{zz} = \chi_\perp/(1 + \chi_\perp g)$. Owing to the linear coupling the orbital order parameter is directly proportional to the anisotropy in the magnetic susceptibility: $\chi_{xx} - \chi_{yy} \propto \psi \propto \sqrt{T_{OO} - T}$ in the vicinity of the ferro-orbital ordering transition.

Now the question arises how such a ferro-orbital ordering affects the Knight shifts $\mathcal{K}_\alpha = A^{hf}_{\alpha\alpha}\chi_{\alpha\alpha}$, where $\alpha = x, y, z$. Owing to the orthorhombic symmetry only the three diagonal terms are present[2]. This is in agreement with the experiments showing $\mathcal{K}_{x,y} \neq \mathcal{K}_z$. It is useful to consider the average, isotropic part of the in-plane Knight shift

$$\mathcal{K}^{av}_{\|a} = A^{hf}_{xx}\chi_{xx} + A^{hf}_{yy}\chi_{yy} = 1/2(A^{hf}_{xx} + A^{hf}_{yy})(\chi_{xx} + \chi_{yy}) + 1/2(A^{hf}_{xx} - A^{hf}_{yy})(\chi_{xx} - \chi_{yy})$$

separately from the difference, the anisotropic in-plane Knight shift

$$\Delta\mathcal{K}_{\|a} = A^{hf}_{xx}\chi_{xx} - A^{hf}_{yy}\chi_{yy} = 1/2(A^{hf}_{xx} + A^{hf}_{yy})(\chi_{xx} - \chi_{yy}) + 1/2(A^{hf}_{xx} - A^{hf}_{yy})(\chi_{xx} + \chi_{yy})$$

An analysis of the hyperfine constants establishes that $A^{hf}_{xx} - A^{hf}_{yy} \propto \psi$, so that $\Delta\mathcal{K}_{\|a} \propto \psi \propto \sqrt{T_{OO} - T}$. Thus, the anisotropic Knight shift is directly proportional to the orbital ordering parameter but the same analysis shows that $K^{av}_{\|a}$ and K_z may depend on ψ only in higher order.

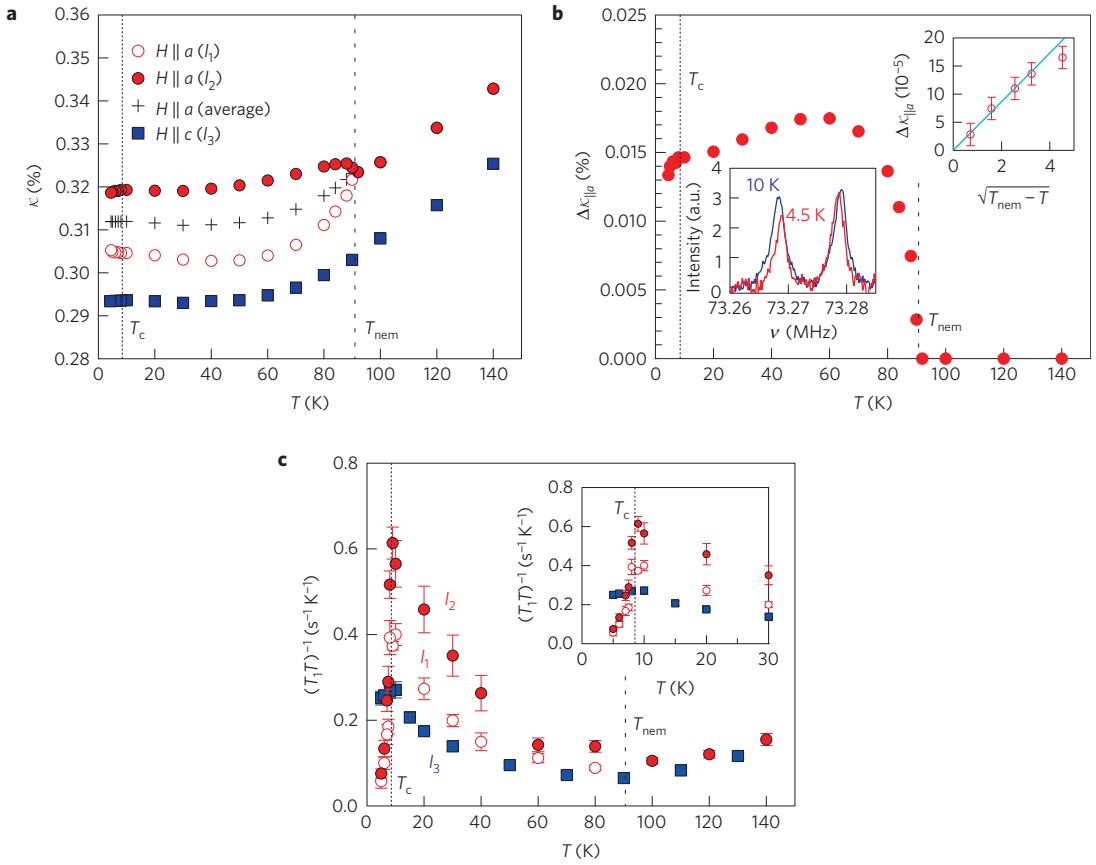

Figure 3 | Emergence of orbital-driven nematic state in FeSe. a, Temperature dependence of the ^{77}Se NMR Knight shift $\mathcal{K}$ for fields $\|a$ and $\|c$. Whereas at T_{nem}, $\mathcal{K}_{\|a}$ splits into lines l_1 and l_2, both $\mathcal{K}_{\|c}$ and $\mathcal{K}^{av}_{\|a}$, the average position of lines l_1 and l_2, show a smooth T-dependence. **b**, Temperature dependence of the l_1–l_2 line splitting below T_{nem} in terms of the difference in Knight shift $\Delta\mathcal{K}_{\|a}$. Insets: (upper right) below T_{nem} the splitting $\Delta\mathcal{K}_{\|a}$ is proportional to $\sqrt{T_{nem}-T}$, as is expected for an order parameter at a second-order phase transition; (lower left) the comparison of two ^{77}Se spectra at 10 K ($> T_c$) and 4.5 K ($< T_c$) reveals that the splitting between the l_1 and l_2 lines clearly decreases in the superconducting state. The intensities of two spectra were normalized for comparison. **c**, Temperature dependence of the spin-lattice relaxation rate divided by T, $(T_1T)^{-1}$. The error bars reflect the uncertainty in the fitting procedure. At around T_{nem} the spin-relaxation rate barely changes, indicating the absence of a magnetic instability. Approaching T_c enhances $(T_1T)^{-1}$, signalling that AFM spin fluctuations develop. Below T_c, as is conventional in the superconducting state, $(T_1T)^{-1}$ strongly drops. The inset shows an enlargement of the low-temperature regime.

We can now compare the theoretical analysis for an orbital-driven nematic state with our experimental results. Clearly the measured splitting $\Delta\mathcal{K}_{\|a}$ shows the $\sqrt{T_{nem}-T}$ behaviour close to the critical temperature, so that we conclude that $T_{nem} = T_{OO}$. At the same time the measured $\mathcal{K}^{av}_{\|a}$ and $\mathcal{K}_{\|c}$ (Fig. 3a) indeed barely show an anomaly in their temperature dependence. In the normal state, between ~50–60 K and T_c the splitting $\Delta\mathcal{K}_{\|a}$ decreases. This is due to the two distinct contributions to $\Delta\mathcal{K}_{\|a}$: the temperature dependence of the hyperfine constant $A^{hf}_{xx} - A^{hf}_{yy}$ and of the susceptibility $\chi_{xx} - \chi_{yy}$. The former saturates below 50–60 K, as the nematic order parameter tends to a constant[25]. At the same time the anisotropic part of the transverse susceptibility changes owing to non-Fermi liquid effects caused by the enhanced spin fluctuations[28], leading to the observed decrease in $\Delta\mathcal{K}_{\|a}$ in the normal state. The issue that remains open from the NMR data is the precise pattern of orbital ordering that is formed. The NMR data do not fix the directions of x and y with respect to the crystallographic axes. Any rotation of the FOO ordering pattern around the c axis is therefore possible in principle. However, the orthorhombic lattice distortion induced by the FOO ordering leaves all Fe–Se distances equivalent[6], which implies that $x \| a$ and $y \| b$, leading to the FOO pattern in Fig. 4.

The conclusion above, that below T_{nem} the orbital order as shown in Fig. 4 renders the electronic structure along the a and b direction inequivalent, resulting in clearly different NMR responses for $H \| a$ and $H \| b$, can be tested. When the magnetic field is applied in the ab plane in the diagonal direction, that is, $H \| [110]$, the field has equal projections on a and b (see Fig. 4). Therefore, the two domains in our twinned crystal should now yield the same NMR response, implying that for this field orientation the splitting between l_1 and l_2 in the orthorhombic state below T_{nem} should be absent. We performed the experiment with $H \| [110]$, using a different single-crystalline platelet glued in the required orientation. As shown in Fig. 2b now a splitting of the line below T_{nem} is indeed clearly absent, which is direct proof that below T_{nem} the rotational (C4) symmetry is broken. We note that our NMR experiments do not provide information on the size of the domains, which might in principle be ordered or disordered at a microscopic scale, which implies the presence of a certain amount of antiferro-orbital ordering. The relevance of such secondary orderings might be probed by NMR experiments on detwinned crystals.

Having established that orbital order drives the nematic ordering, the question arises how the orbital ordering affects not only the lattice and spin degrees of freedom, but also the superconducting state. The relation to the secondary orthorhombic lattice distortion has been discussed above. From the NMR data also the coupling between the orbital order to the spin degrees of freedom is directly evident. The spin–lattice relaxation rate, measuring the strength of low-energy spin fluctuations, shows that in the vicinity of T_{nem}

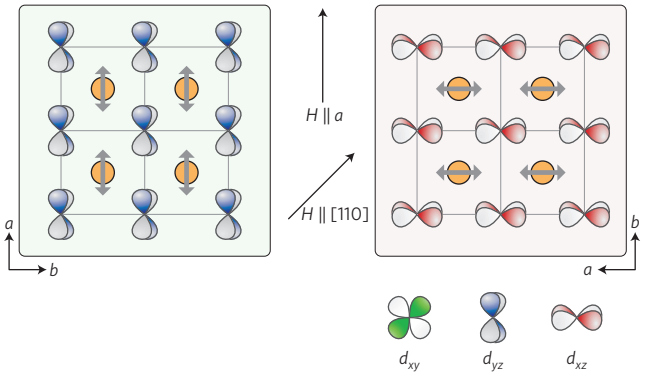

Figure 4 | Top view of the FOO in FeSe with the two different domains that are present in a twinned crystal. The three orthogonal orbitals d_{xy}, d_{yz} and d_{xz} are indicated. The double-headed arrows indicate the nematic order parameter.

there is little, if any, enhancement of the magnetic excitations, an enhancement that would be expected from Fermi-liquid theory in the vicinity of a spin-density wave transition. This implies that the characteristic energy of the degrees of freedom driving the nematic transition considerably differs from the characteristic energy of magnetic degrees of freedom: orbital and spin degrees of freedom are well separated. When going below T_{nem} the spin–lattice relaxation rate increases steadily, approaching T_c in a manner that is quantitatively different for the lines l_1 and l_2 (see Fig. 3c). This is to be expected because the spin-relaxation rate in the FOO state picks up the anisotropies in its hyperfine couplings and susceptibilities, as the Knight shift does.

Finally, we analyse the interplay of the orbital ordering and superconductivity. Previously, scanning tunnelling spectroscopy measurements have found a two-fold breaking of the Cooper-pair symmetry in FeSe, which implies that the superconducting order parameter is directly affected by the nematicity[29]. Here we observe the complementary effect: the splitting $\Delta\mathcal{K}_{\|a}$ (which is proportional to the orbital order parameter) changes significantly below T_c (see Supplementary Methods). Thus, the nematic order parameter is directly affected by superconductivity. The splitting $\Delta\mathcal{K}_{\|a}$ becoming smaller while the Knight shifts $\mathcal{K}_{\|c}$ and $\mathcal{K}^{av}_{\|a}$ barely change indicates that in our bulk FeSe crystals superconductivity and nematicity compete—superconductivity tends to suppress orbital ordering and vice versa. It is interesting to note that in the single layers of FeSe for which spectacularly high T_c values have been reported[19–24] a tetragonal–orthorhombic transition is absent, evidencing a much weaker nematic tendency. It will have to be established whether the suppressed nematicity is a cause for the strongly enhanced T_c in FeSe single layers.

Methods

Single crystals of FeSe ($T_c \sim 9.3$ K) were grown using a KCl–$AlCl_3$ flux technique as described in detail elsewhere[30]. The mixture of Fe, Se, $AlCl_3$ and KCl was sealed in an evacuated Pyrex ampoule. The samples were heated to 450 °C in a horizontal tube furnace, held at this temperature for 40 days. The temperature of the hottest part of the ampoule was 450 °C and the coolest part was 370–380 °C. The obtained product was washed with distilled water to remove flux and other by-products and then the tetragonal-shaped single crystals were mechanically extracted. The typical size of the obtained crystals was $1 \times 1 \times 0.1$ mm^3. The temperature dependence of the resistivity of FeSe single crystals was measured using a conventional four-probe configuration in a 14 T physical property measurements system and the magnetic susceptibility was measured in a 5 T magnetic property measurements system.

^{77}Se (nuclear spin $I = 1/2$) NMR was carried out in a FeSe single crystal ($0.7 \times 0.7 \times 0.1$ mm^3) at an external field of 9 T and in the range of temperature 4.2–140 K. The sample was rotated using a goniometer for the exact alignment along the external field. The ^{77}Se NMR spectra were acquired by a standard spin-echo technique with a typical $\pi/2$ pulse length 2–3 μs. The nuclear spin–lattice relaxation rate T_1^{-1} was obtained by fitting the recovery of the nuclear magnetization $M(t)$ after a saturating pulse to a single exponential function, $1 - M(t)/M(\infty) = A\exp(-t/T_1)$, where A is a fitting parameter.

Received 29 July 2014; accepted 9 October 2014; published online 10 November 2014

References

1. Yi, M. *et al.* Symmetry-breaking orbital anisotropy observed for detwinned $Ba(Fe_{1-x}Co_x)_2As_2$ above the spin density wave transition. *Proc. Natl Acad. Sci. USA* **108,** 6878–6883 (2011).
2. Chu, J-H., Kuo, H-H., Analytis, J. G. & Fisher, I. R. Divergent nematic susceptibility in an iron arsenide superconductor. *Science* **337,** 710–712 (2012).
3. Kasahara, S. *et al.* Contrasts in electron correlations and inelastic scattering between LiFeP and LiFeAs revealed by charge transport. *Phys. Rev. B* **85,** 060503 (2012).
4. Böhmer, A. E. *et al.* Nematic susceptibility of hole-doped and electron-doped $BaFe_2As_2$ iron-based superconductors from shear modulus measurements. *Phys. Rev. Lett.* **112,** 047001 (2014).
5. McQueen, T. M. *et al.* Tetragonal-to-orthorhombic structural phase transition at 90 K in the superconductor $Fe_{1.01}Se$. *Phys. Rev. Lett.* **103,** 057002 (2009).
6. Margadonna, S. *et al.* Crystal structure of the new $FeSe_{1-x}$ superconductor. *Chem. Commun.* 5607–5609 (2008).
7. Fu, M. *et al.* NMR search for the spin nematic state in a LaFeAsO single crystal. *Phys. Rev. Lett.* **109,** 247001 (2012).
8. Fang, C., Yao, H., Tsai, W-F., Hu, J. & Kivelson, S. A. Theory of electron nematic order in LaFeAsO. *Phys. Rev. B* **77,** 224509 (2008).
9. Xu, C. & Sachdev, S. The new iron age. *Nature Phys.* **4,** 898–900 (2008).
10. Fradkin, E. & Kivelson, S. A. Electron nematic phases proliferate. *Science* **327,** 155–156 (2010).
11. Krüger, F., Kumar, S., Zaanen, J. & van den Brink, J. Spin-orbital frustrations and anomalous metallic state in iron-pnictide superconductors. *Phys. Rev. B* **79,** 054504 (2009).
12. Lv, W., Wu, J. & Phillips, P. Orbital ordering induces structural phase transition and the resistivity anomaly in iron pnictides. *Phys. Rev. B* **80,** 224506 (2009).
13. Lee, C-C., Yin, W-G. & Ku, W. Ferro-orbital order and strong magnetic anisotropy in the parent compounds of iron-pnictide superconductors. *Phys. Rev. Lett.* **103,** 267001 (2009).
14. Daghofer, M. *et al.* Orbital-weight redistribution triggered by spin order in the pnictides. *Phys. Rev. B* **81,** 180514 (2010).
15. Chen, C-C. *et al.* Orbital order and spontaneous orthorhombicity in iron pnictides. *Phys. Rev. B* **82,** 100504 (2010).
16. Fernandes, R. M., Chubukov, A. V. & Schmalian, J. What drives nematic order in iron-based superconductors? *Nature Phys.* **10,** 97–104 (2014).
17. Paglione, J. & Greene, R. L. High-temperature superconductivity in iron-based materials. *Nature Phys.* **6,** 645–658 (2010).
18. Hsu, F-C. *et al.* Superconductivity in the PbO-type structure α-FeSe. *Proc. Natl Acad. Sci. USA* **105,** 14262–14264 (2008).
19. Wang, Q-Y. *et al.* Interface-induced high-temperature superconductivity in single unit-cell FeSe films on $SrTiO_3$. *Chin. Phys. Lett.* **29,** 037402 (2012).
20. Xiang, Y-Y., Wang, F., Wang, D., Wang, Q-H. & Lee, D-H. High-temperature superconductivity at the FeSe/$SrTiO_3$ interface. *Phys. Rev. B* **86,** 134508 (2012).
21. Tan, S. *et al.* Interface-induced superconductivity and strain-dependent spin density waves in FeSe/$SrTiO_3$ thin films. *Nature Mater.* **12,** 634–640 (2013).
22. He, S. *et al.* Phase diagram and electronic indication of high-temperature superconductivity at 65 K in single-layer FeSe films. *Nature Mater.* **12,** 605–610 (2013).
23. Zhang, W-H. *et al.* Direct observation of high-temperature superconductivity in one-unit-cell FeSe films. *Chin. Phys. Lett.* **31,** 017401 (2014).
24. Ge, J-F. *et al.* Superconductivity in single-layer films of FeSe with a transition temperature above 100 K. Preprint at http://arxiv.org/abs/1406.3435 (2014).
25. Böhmer, A. E. *et al.* Lack of coupling between superconductivity and orthorhombic distortion in stoichiometric single-crystalline FeSe. *Phys. Rev. B* **87,** 180505 (2013).
26. Imai, T., Ahilan, K., Ning, F. L., McQueen, T. M. & Cava, R. J. Why does undoped FeSe become a high-T_c superconductor under pressure? *Phys. Rev. Lett.* **102,** 177005 (2009).
27. Medvedev, S. *et al.* Electronic and magnetic phase diagram of β-$Fe_{1.01}Se$ with superconductivity at 36.7 K under pressure. *Nature Mater.* **8,** 630–633 (2009).
28. Korshunov, M. M., Eremin, I., Efremov, D. V., Maslov, D. L. & Chubukov, A. V. Nonanalytic spin susceptibility of a fermi liquid: The case of Fe-based pnictides. *Phys. Rev. Lett.* **102,** 236403 (2009).

29. Song, C-L. *et al.* Direct observation of nodes and twofold symmetry in FeSe superconductor. *Science* **332,** 1410–1413 (2011).
30. Chareev, D. *et al.* Single crystal growth and characterization of tetragonal $FeSe_{1-x}$ superconductors. *Cryst. Eng. Commun.* **15,** 1989–1993 (2013).

Acknowledgements

The authors thank G. Prando and H-J. Grafe for discussion. This work has been supported by the Deutsche Forschungsgemeinschaft (Germany) through DFG Research Grants BA 4927/1-1 and the Priority Program SPP 1458. Financial support through the DFG Research Training Group GRK 1621 is gratefully acknowledged. The work at POSTECH was supported by the National Research Foundation (NRF) through the Mid-Career Researcher Program (No. 2012-013838), SRC Center for Topological Matter (No. 2011-0030046), and the Max Planck POSTECH/KOREA Research Initiative Program (No. 2011-0031558), and also by the Institute of Basic Science (IBS) through the Center for Artificial Low Dimensional Electronic Systems.

Author contributions

S-H.B. performed the main NMR measurements, analysed data, and participated in writing of the manuscript; J.M.O. and J.S.K. synthesized the sample; D.V.E. and J.v.d.B. provided theoretical support and participated in writing of the manuscript; B.B. supervised and guided the study and participated in the writing of the manuscript. All authors discussed the results and commented on the manuscript.

Additional information

Supplementary information is available in the online version of the paper. Reprints and permissions information is available online at www.nature.com/reprints. Correspondence and requests for materials should be addressed to S-H.B.

Competing financial interests

The authors declare no competing financial interests.